Tunable Fiber-Optic Delay Line Based on Stimulated Brillouin Scattering

Weiwen Zou, Zuyuan He, and Kazuo Hotate

Department of Electrical Engineering and Information Systems, The University of Tokyo, Bunkyo, Tokyo 113-8656, Japan

Received November 17, 2009; accepted December 6, 2009; published online December 25, 2009

We demonstrate a novel method to build a tunable fiber-optic delay line based on stimulated Brillouin scattering (SBS) in a single-mode optical fiber. The frequency of a continuous-wave lightwave served as the Brillouin probe is linearly swept to determine the location in the fiber where a pulse signal served as the Brillouin pump is reflected and thus delayed via SBS-intensified acoustic grating. The novel fiber-optic delay line has a linear tunability of more than 4 μs. The pulse distortion is also studied. © 2010 The Japan Society of Applied Physics

DOI: 10.1143/APEX.3.012501

A fiber-optic delay line is one of the key components for all-optical processing in telecom networks and for optical buffering or storage. By cascading a series of fiber Bragg gratings at different wavelengths, Ball *et al.* developed a delay line for optical pulse signals.[1)] This method, however, can generate only invariable and discrete time delays. Several concepts were recently demonstrated to obtain a tunable delay line.[2–6)] Comparably, the method[2–4)] using Brillouin slow light can realize a tunable delay line at an arbitrary optical wavelength. In Brillouin slow light, the pulse signal served as the Brillouin probe is launched into an optical fiber to obtain Brillouin amplification from a strong Brillouin pump through stimulated Brillouin scattering (SBS) effect, and thus the group velocity of the pulse signal is slowed. The time delay is proportional to the Brillouin gain accumulated along the entire optical fiber. Due to the effective length of the optical fiber and the power depletion of the pump wave, the achievable Brillouin gain is limited. Furthermore, more serious pulse distortion is induced by stronger Brillouin amplification. Therefore, the obtainable time delay is typically confined within few pulse widths.[2,3)]

In this paper, we demonstrate a novel method to build a SBS-based fiber-optic delay line. The principle is completely different from the concept of Brillouin slow light.[2,3)] The optical pulse signal served as the Brillouin pump is reflected and delayed by the SBS-intensified acoustic grating at a particular location in the fiber. The reflection location is determined by a counter-propagating continuous-wave (cw) lightwave served as the Brillouin probe, which is linearly frequency-modulated. The novel fiber-optic delay line has a linear tunability of more than 4 μs. The physical principle, the experimental demonstration, and the discussion on the pulse distortion are presented.

The principle of the proposed fiber-optic delay line is schematically depicted in Fig. 1. A pulse signal enters an optical fiber in $+z$ direction. The pulse signal is continuously reflected along the entire fiber, producing weak pulses originated from Rayleigh scattering and Stokes or anti-Stokes in spontaneous Brillouin scattering (SpBS).[7)] The reflected pulses are time-dependent or position-dependent. On the other hand, a cw lightwave is incident into the opposite end in $-z$ direction as the control light. The frequency of the cw control light is linearly swept as $f(t) = f_{cw} - \Delta f/T \cdot t$, where f_{cw} is the initial frequency at $t = 0$, Δf the modulation depth, and T the modulation period, respectively. Thus, the pulse signal encounters the cw control light with different optical frequency $f(z)$ at different position z. The $f(z)$ is expressed by

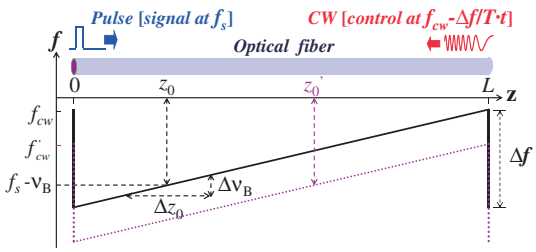

Fig. 1. Principle of the proposed SBS-based fiber-optic delay line. A pulse signal and a cw control light are counter-propagated along an optical fiber. The control light is linearly frequency-modulated to determine the location (z_0) where SBS occurs and the pulse signal is delayed. Decreasing the initial frequency of the cw control light from f_{cw} to f'_{cw} can shift the SBS-occurring location from z_0 to z'_0.

$$f(z) = f_{cw} + \Delta f \cdot \frac{z - L}{L}, \tag{1}$$

where $L = T \cdot v_g$ and v_g is the light group velocity.

Within the L-length fiber, there is only one location (z_0) at which the cw control light satisfies the phase-matching condition $f(z_0) = f_s - \nu_B$, where ν_B is the Brillouin frequency shift and f_s the frequency of the pulse signal, respectively. The location z_0 is determined by $z_0 = [(f_s - \nu_B) - f_{cw}] \cdot L/\Delta f + L$. It is notable that the repetition period of the pulse should be equal to the modulation period T. Only at the location z_0, the weak Stokes pulse is amplified due to the SBS effect between the pulse and the cw light. Therefore, the pulse signal is strongly reflected and delayed by

$$t_0 = 2 \cdot \frac{z_0}{v_g} = 2[(f_s - \nu_B) - f_{cw}] \cdot \frac{T}{\Delta f} + 2T, \tag{2}$$

where the coefficient 2 is due to the round-trip propagation.

As schematically shown in Fig. 1, the SBS-occurring location z_0 can be shifted to z'_0 by decreasing the initial frequency of the cw control light from f_{cw} to f'_{cw} while the other modulation parameters (Δf and T) are fixed. So, the time delay (t_0) can be tuned. According to eq. (2), the tunable rate ($k = \delta t_0/\delta f_{cw}$) is linearly given by

$$k = -\frac{2T}{\Delta f}. \tag{3}$$

We assume that the bandwidth of the pulse signal is narrower than the intrinsic Brillouin linewidth ($\Delta\nu_B \simeq 40$ MHz). Due to the linear frequency-sweeping of the cw control light, the Brillouin amplification occurs within a spatial zone (Δz_0) around the location z_0 as shown in Fig. 1. The spatial zone is decided by $\Delta z_0 = \Delta\nu_B \cdot T \cdot v_g/\Delta f$. The spatial zone determines the Brillouin interaction length. The

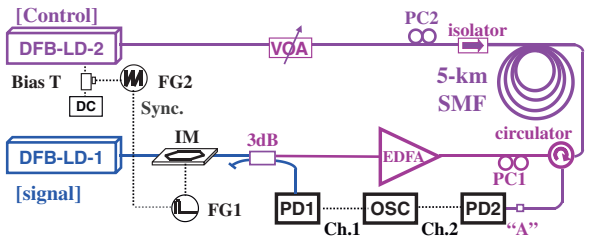

Fig. 2. Experimental setup. Distributed-feedback laser diode (DFB-LD); intensity modulator (IM); variable optical attenuator (VOA); polarization controller (PC); erbium-doped fiber amplifier (EDFA); single-mode optical fiber (SMF); function generator (FG); photo-diode (PD); oscilloscope (OSC).

optical power of the delayed pulse (P_d) can be approximately estimated by

$$P_d = P_{cw} \cdot e^{g \cdot P_s \cdot \Delta z_0} \simeq P_{cw} + \frac{g P_{cw} P_s \Delta \nu_B T v_g}{\Delta f}, \quad (4)$$

where P_{cw} is the optical power of the cw light, and P_s that of the pulse signal, respectively; g is the normalized Brillouin gain coefficient determined by the fiber material and structure, and the mutual polarization states between the pulse signal and the cw control light.[7)]

Furthermore, the shape of the delayed pulse is reshaped into a Lorentz-like profile with a full width at half maximum (FWHM, τ') related to the spatial zone as

$$\tau' = \frac{2\Delta z_0}{v_g} = \Delta \nu_B \cdot \left(\frac{2T}{\Delta f}\right). \quad (5)$$

Note that eq. (5) is effective only if the value of τ' is greater than that of τ'' decided by the intrinsic Brillouin linewidth as

$$\tau'' = \Delta \nu_B{}^{-1}. \quad (6)$$

The experimental setup is illustrated in Fig. 2. The delay-line medium is a 5-km standard single-mode optical fiber (SMF) corresponding to one-way light transit time of ~25 μs. A 1549-nm distributed-feedback laser diode (DFB-LD-1) with ~2-MHz linewidth works as the light source of the pulse signal to be delayed. A function generator (FG1) and an intensity modulator (IM) are used to generate a rectangular optical pulse. The pulse width (~80 ns) and repetition period (~50 μs) are set in order to ensure that the pulse's bandwidth is narrower than $\Delta\nu_B$ and there is only one pulse within the delay-line fiber, respectively. One part of the pulse power is detected by a photo-diode (PD1) and recorded by an oscilloscope (OSC) as a reference. The other part is amplified by an erbium-doped fiber amplifier (EDFA) to ~10 dBm and launched into the SMF through an optical circulator.

The cw control light is provided by the second DFB-LD-2 also with ~2-MHz linewidth. Its initial frequency f_{cw} = 193.570 THz is linearly changeable by tuning its dc injection current (I_{dc} = 110 mA) with 0.01-mA step. The frequency–current tuning rate is measured to be $\Delta f_{cw}\Delta I_{dc} = -0.943$ GHz/mA where Δf_{cw} or ΔI_{dc} is the detuned initial frequency or the detuned dc injection current. The frequency of the cw control light is swept by a saw-tooth waveform from the second function generator (FG2), which is synchronized with the FG1. The saw-tooth waveform has 4.749-μs fall region and 45.251-μs rise region. The entire period (50 μs) of the saw-tooth waveform is chosen to ensure that the pulse signal

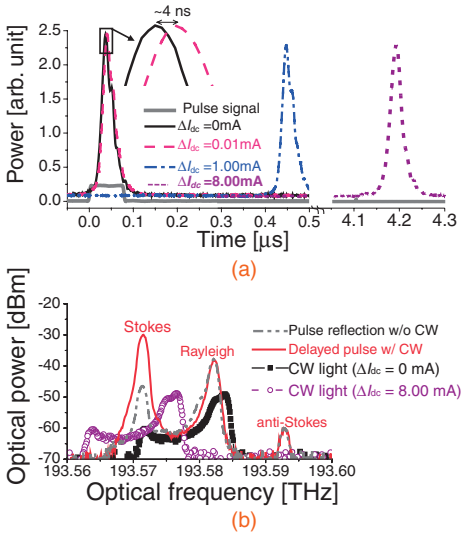

Fig. 3. (a) Typical examples of delayed pulse with different time delay for different detuned dc injection current (ΔI_{dc}). The inset is the magnified plot of the 4-ns delayed pulse. (b) Optical spectra of the cw control light for ΔI_{dc} = 0 or 8.00 mA, the corresponding delayed pulse, and the reflected weak pulses without the cw control light launched.

can encounter the cw control light with different frequency along the entire SMF. A part of the fall region with the length of T = 2.068 μs and the depth of $\Delta f \simeq$ 7.5 GHz is used in this study. The cw control light is attenuated by a variable optical attenuator (VOA) to −30 dBm and is launched into the other end of the SMF through an isolator. At the "A" adapter, the delayed pulse signal is detected by PD2, or measured by an optical spectrum analyzer (OSA), which is not shown in Fig. 2. The polarization states of the pulse signal and the cw control light are mutually optimized to maximize the Brillouin amplification as well as the power of the delayed pulse via polarization controllers (PCs).

Figure 3(a) shows typical examples of the delayed pulse at different ΔI_{dc}, i.e., different Δf_{cw}. The time delay (t_0) is measured to be 0, 4, 420, or 4136 ns corresponding to ΔI_{dc} = 0, 0.01, 1.00, or 8.00 mA, respectively. The magnified plot of the 4-ns delayed pulse is shown in the inset of Fig. 3(a). Figure 3(b) shows the measured optical spectra of the cw control light under different ΔI_{dc} of 0 or 8.00 mA, the corresponding delayed pulse and the reflected weak pulses without the cw control light launched. Comparing the two cases with and without the cw control light launched, we know that the Rayleigh component and SpBS anti-Stokes component keeps almost unchanged, but Stokes component is extensively enhanced due to the SBS effect attributed to the phase-matched cw control light at the delay location [see eq. (4)]. The optical spectrum of the control lights shifting with ΔI_{dc} (Δf_{cw}) is adjusted, while the optical spectrum of the delayed pulse is independent of ΔI_{dc} (Δf_{cw}).

As shown in Fig. 3(a), the delayed pulses all include slight dc levels. The dc levels (i.e., the noise figure) of the delayed pulses are attributed to Rayleigh, SpBS anti-Stokes and SpBS Stokes components as well as the cw control light. Figure 3(b) shows that Rayleigh component is higher than SpBS anti-Stokes component by ~20 dB and higher than SpBS Stokes component by ~6 dB, which means that Rayleigh component has stronger influence on the noise

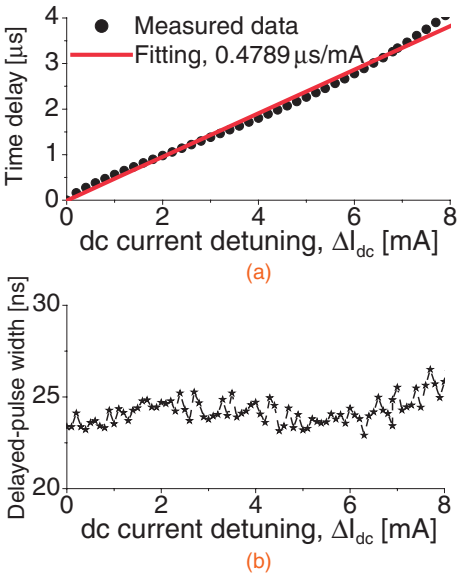

Fig. 4. Dependences of the time delay (a) and the width (b) of the delayed pulse on the dc detuned injection current (ΔI_{dc}) of the control light. Note that the frequency–current tuning rate is experimentally characterized as −0.943 GHz/mA.

figure when compared to SpBS anti-Stokes and SpBS Stokes components. The ratio of the enhanced Stokes component to the Rayleigh component is ∼10 dB, which partially determines the noise figure of the delayed pulses. On the other hand, the influence of the cw control light is even more serious than Rayleigh component. This is because the delayed pulse exists on the top of the base of the cw control light [see eq. (4)]. To further reduce to some extent the influence of the cw control light, the input power of the cw control light is attenuated to be −30 dBm in this study. Further work will be done to clarify the noise figure in detail.

The dependence of the time delay on the dc injection current detuning is also studied. The experimental result is summarized in Fig. 4(a), which shows that the time delay can be linearly tuned by the dc injection current detuning. The least-squares linear fitting to the experimental data gives the tunable rate $k = 0.479\,\mu s/mA$ or $-0.508\,\mu s/GHz$, which matches well with the theoretical value of $-2T/\Delta f = -0.551\,\mu s/GHz$ [see eq. (3)].

According to eqs. (3) and (5), the FWHM of the delayed pulse is determined by the tunable rate k. By inputting the above tunable rate ($k_{10} = -0.551\,\mu s/GHz$) into eq. (5), the FWHM of the delayed pulse is estimated as $\tau' = 40 \times 0.551\,ns \simeq 22\,ns$. However, since the bandwidth of the reflected pulse is about 40 MHz due to the intrinsic Brillouin linewidth, the FWHM of the delayed pulse cannot be smaller than $\tau'' = 25\,ns$ according to eq. (6). As depicted in Fig. 4(b), the FWHM of each delayed pulse is measured around 23–26 ns, which agrees well with the above theoretical estimation provided that the measurement accuracy (±2 ns) is taken into account. When the input pulse width (τ_0) varies from 30 to 320 ns, the FWHM of the delayed pulse is almost the same because the bandwidth of the Brillouin amplification is inherently decided by the intrinsic Brillouin linewidth.

Moreover, we investigate the influence of the modulation depth Δf of the cw control light. Other parameters of the cw control light and the input pulse signal are fixed at $T = 2.068\,\mu s$, $\Delta I_{dc} = 1.00\,mA$, and $\tau_0 = 80\,ns$, respectively. When the modulation depth Δf is increased, the power of the delayed pulse is decreased, as shown in Fig. 5(a). This is because the Brillouin interaction length is reduced and thus the reflected power is consequently weakened [see eq. (4)].

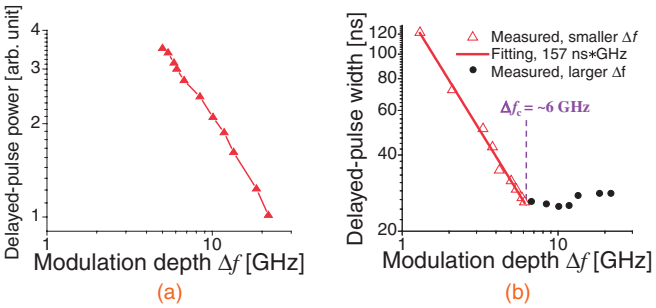

Fig. 5. Dependences of the power (a) and the width (b) of the delayed pulse on the linear modulation depth (Δf) of the cw control light. The dashed line in (b) corresponds to the critical modulation depth $\Delta f_c \simeq 6$ GHz.

The FWHM of the delayed pulse (τ') as a function of the modulation depth Δf is summarized in Fig. 5(b), which shows two different cases as indicated in eqs. (5) and (6), respectively. Between the two cases, there is a critical condition of $\Delta f_c = \Delta\nu_B^2 \cdot 2T \simeq 6.4\,GHz$, which is decided by $\tau' = \tau''$. The measured Δf_c is about 6 GHz and agrees with the theoretical value. When the modulation depth Δf is increased until the critical Δf_c, the SBS-occurring spatial zone is shortened and the pulse width is correspondingly reduced. The linearly-fitted slope of $d\tau'/d\Delta f^{-1} = 157$ ns·GHz matches well with the calculated value of 166 ns·GHz according to eq. (5). For the larger modulation depth over the critical Δf_c, the FWHM of the delayed pulse is maintained around 25–28 ns. This is due to the intrinsic Brillouin linewidth as explained above.

In conclusion, we have theoretically and experimentally demonstrated a novel SBS-based fiber-optic delay line. With a frequency-modulated laser diode as the control light, a standard SMF spool as the delay-line medium, and an optical circulator as the input/output port, as illustrated in purple in Fig. 2, we obtained tunable time delay of 0–4 μs. The minimum tunable time delay of ∼4 ns is limited by the minimum detuned dc injection current of the control light. The tunable range can be further increased by enlarging the modulation period of the control light. The frequency of the delayed pulse is down-shifted by the BFS $\nu_B \simeq 10.87$ GHz of the SMF (the delay-line medium). The delayed pulse is reshaped into a Lorentz-like profile. The pulse width can be maintained by properly designed modulation parameters, especially the modulation depth.

Acknowledgments This work was supported by a Grant-in-Aid for Scientific Research (S) and the Global Center of Excellence Program from the Ministry of Education, Culture, Sports, Science and Technology, Japan (MEXT).

1) G. A. Ball *et al.*: IEEE Photonics Technol. Lett. **6** (1994) 741.
2) K. Y. Song *et al.*: Opt. Express **13** (2005) 82.
3) Y. Okawachi *et al.*: Phys. Rev. Lett. **94** (2005) 153902.
4) K. Y. Song and K. Hotate: Opt. Lett. **32** (2007) 217.
5) J. Sharping *et al.*: Opt. Express **13** (2005) 7872.
6) J. B. Khurgin and P. A. Morton: Opt. Lett. **34** (2009) 2655.
7) R. W. Tkach and A. R. Chraplyvy: Opt. Quantum Electron. **21** (1989) S105.